RESEARCH PROGRESS IN MECHANICAL AND MANUFACTURING ENGINEERING
e-ISSN: 2773-4765

RPMME

Vol. 6 No. 1 (2025) 51-64
https://publisher.uthm.edu.my/periodicals/index.php/rpmme

Fabrication of Filament PLA and PLA/HAp

Jerome Tunggat anak Kasin[1], Maizlinda Izawana Idris[2]*

[1] *Department of Mechanical & Manufacturing Engineering, University Tun Hussein Onn Malaysia, Batu Pahat, 86400 Parit Raja,Johor, Malaysia*
[2] *Bioactive Materials (BioMa) Centre of Research, Faculty of Mechanical & Manufacturing Engineering, Universiti Tun Hussein Onn Malaysia, Batu Pahat, 86400 Parit Raja,Johor, Malaysia*

*Corresponding Author: izwana@uthm.edu.my
DOI: https://doi.org/10.30880/rpmme.2025.06.01.006

Article Info

Received: 2 February 2025
Accepted: 24 April 2025
Available online: 31 July 2025

Keywords

PLA, Hydroxyapatite, Filemants, Biomedical, Charaterization, SEM, AFM, FTIR, UTM

Abstract

3D printing or additive manufacturing (AM) transforms digital designs into physical objects by layering material sequentially, enabling the creation of complex forms with reduced material waste. Polylactic acid (PLA), a biodegradable and nontoxic material derived from renewable resources, is the most used filament in Fused Deposition Modelling (FDM) due to its ease of use and wide compatibility. Despite its theoretical composability, PLA requires industrial composting facilities for proper degradation. This research aims to fabricate PLA/HAp filaments through the extrusion method and investigate their mechanical, physicochemical, and structural properties. Comprehensive characterization of PLA and PLA/HAp filaments will be conducted to evaluate their potential for advanced additive manufacturing applications. The methodology involves the preparation of high-quality PLA and PLA/HAp filaments through precise extrusion processes, followed by comprehensive analysis of their microstructure, chemical bonding, surface roughness, and mechanical properties. The surface roughness is very crucial, and the highest Roughness Average (Ra) can be found in composition of 70:30 which is 68.974 mm. Modern techniques such as SEM-EDS, FTIR, AFM, and various mechanical tests are utilized to evaluate the quality and potential biomedical applications of the filaments. FTIR, AFM, and SEM-EDS analyses confirm the successful integration of HAp into PLA, revealing increased surface roughness and enhanced mechanical properties with higher HAp content. Tensile, flexural, and bending tests demonstrate improved strength and modulus, indicating the potential of PLA/HAp composites for advanced biomedical applications. This study investigates the mechanical properties, characterization, and physiochemical analysis of PLA/HAp filaments, highlighting their potential in medical applications. FTIR analysis confirmed successful chemical bonding between PLA and HAp, crucial for applications such as tissue engineering and orthopedic implants. Surface roughness and microstructural analyses revealed enhanced properties in PLA/HAp composites, with significant improvements in mechanical strength and biocompatibility.

1. Introduction

The fabrication of PLA and PLA/HAp filaments represents a significant advancement in materials science, particularly in additive manufacturing and biomedical engineering. Polylactic Acid (PLA), a biodegradable and biocompatible polymer derived from renewable resources, serves as an environmentally friendly alternative to traditional plastics. When combined with Hydroxyapatite (HAp), a naturally occurring mineral that promotes bone growth, the resulting PLA/HAp composites exhibit enhanced mechanical properties and bioactivity. These attributes make them particularly suitable for applications in tissue engineering, medical implants, and other biomedical devices. Despite the promising nature of PLA and HAp composites, there remains a lack of thorough understanding of the interactions within PLA/HAp filaments. It is crucial to evaluate PLA's independent performance in scenarios where HAp's enhanced mechanical properties may not be necessary. This thesis explores the methodologies for producing these innovative filaments, evaluates their material properties, and assesses their potential for various applications, aiming to determine the optimal blending ratios and processing conditions to create PLA/HAp composites tailored for biomedical applications [1].

2. Materials and methods

This chapter will give insight regarding the preparation of materials and characterization of PLA, HAp and three compositions of PLA/HAp.

2.1 Material preparation

Table 1 shows the composition of PLA/HAp will be used throughout this study.

Table 1 *Composition of PLA/HAp*

No. of item	Weight ratio ($wt.\%$)
1	90/10
2	80/20
3	70/30

2.2 Methods

For the fabrication of the PLA/HAp biocomposites filaments, Hydroxyapatite particles are added into the PLA matrix during the fabrication of PLA/HAp (Polylactic Acid/Hydroxyapatite) biocomposite filaments to improve its characteristics, particularly for use in biomedicine and tissue engineering.

Select high-quality PLA pallets and natural hydroxyapatite. *Fringescale* sardinella waste including bones was collected and frozen. The bones were thawed and boiled for an hour to inactivate enzymes. Next, wash with water under strong pressure to rinse off any other unwanted impurities or protein. Bones were oven-dried at 100°C for 24 hours after cleaning process is done. Milled to reduce size dried bones were rotor milled and were subsequently ball milled to produce a finer HA powder.

The particle size was less than 90 μm by sieve technique, HA powder finally subjected to thermal treatment at several different temperatures in an atmospheric sintering furnace.

To get a better result, drying the PLA beads is essential to remove any moisture and ensure proper extrusion. Hydroxyapatite is typically heat-treated to remove any absorbed water as well. Mix the dried PLA beads with the hydroxyapatite particles with the weight ratio of 90:10, 80:20 and 70:30. The blending process aims to achieve a homogeneous distribution of hydroxyapatite particles within the PLA matrix.

In agreement with previous study, the extruder will be preheated to 167°C as it is the melting point of the PLA/HAp [2]. Then, PLA/HAp mixture was blended followed by extruded via a 1.75+0.5 mm nozzle. The extruder melts the composite and forces it through a die to form a continuous filament. Extrusion parameters, such as temperature and screw speed, are carefully controlled. The composite filament that has been manufactured will have a diameter of 1.75+0.5 mm.

The extruded filament is rapidly cooled to solidify it. Proper cooling is critical to maintain the desired filament diameter and prevent deformities. The PLA/HAp filament is coiled into spools once it has been sized. To avoid tangling and guarantee user-friendliness, the winding procedure must be consistent. Fig. 1 illustrates the schematic diagram fabrication process of PLA/HAp filament.

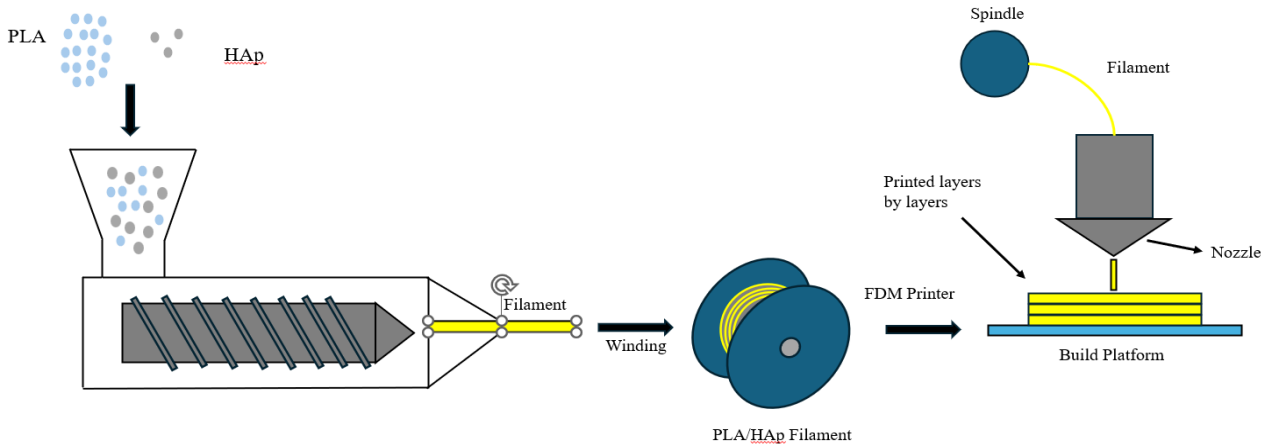

Fig. 1 schematic diagram fabrication process of PLA/HAp filament

2.3 Characterization Process

Fourier Transform Infrared Spectroscopy (FTIR) is used to study the chemical bonding of PLA/HAp because it provides important information that are very crucial in biomedical implants. It was performed using a Perkin Elmer Spectrum 100.

Fig. 2 Fourier Transform Infrared Spectroscopy (FTIR) Perkin Elmer Spectrum 100, United States

Non-Contact Atomic Force Microscopy (NC-AFM) was utilized to examine the topography of PLA, HAp, and three distinct compositions of PLA mixed with 10%, 20%, and 30% HAp. The images were acquired using an XE-100 microscope from Park Systems, Korea. The data that obtained in-depth understanding of the surface roughness of PLA/HAp composites, which is essential for enhancing their effectiveness in biomedical applications.

Fig. 3 Non-Contact Atomic Force Microscopy (NC-AFM) from Park Systems, Korea

UTM is utilized in analyzing the tensile strength of PLA/HAp composites due to their ability to offer precise and controlled environments for assessing mechanical properties. UTM able to give accurate application and measurement of tensile forces, facilitating the determination of the material's maximum strength and elongation prior to failure. This data is vital for evaluating the mechanical behavior and applicability of PLA/HAp composites in biomedical fields, ensuring they can endure the necessary forces in real-world scenarios.

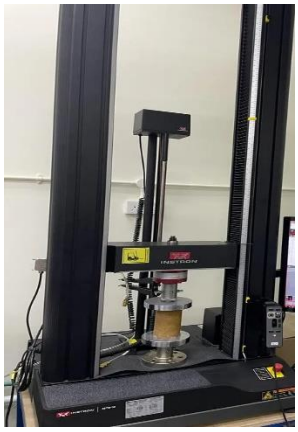

Fig. 4 Universal Testing Machine (UTM)

Scanning Electron Microscope (SEM) with an SU 1510 model, equipped with an Energy Dispersive Spectroscopy (EDS) module, was utilized to assess the distribution of HAp within the polymer matrix for homogeneity. SEM-EDS analysis was conducted on the cross-section of the samples to examine the uniform microstructure of Virgin PLA, HA, and PLA/HAp.

Fig. 5 Scanning Electron Microscope with Electron Dispersive Spectroscopy (SEM-EDS) SU 1510 model, Germany

3. Result and Discussion

Table 3 shows the PLA/HAp in pellets form.

Table 3 *PLA/HAp pellets in pellets form*

Ratio	Results
90:10	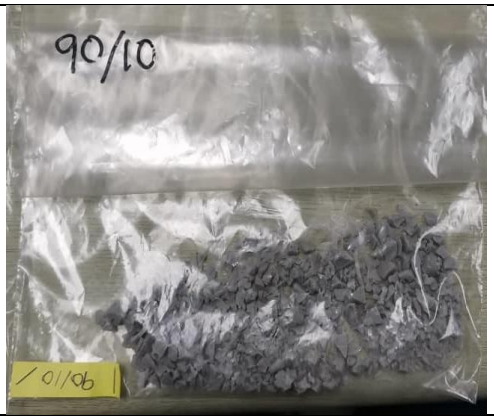

80:20			
70:30			

3.1 Analysis of Chemical Bonding

Fourier Transform Infrared Spectroscopy (FTIR) analysis was performed on each sample to analyze their chemical bonding. It was performed using a Perkin Elmer Spectrum 100. The spectra for each sample were set in a frequency range of 600 – 4,000 cm^{-1}. The spectra of FTIR results were plotted as percent transmittance (%T) versus wavenumber (cm^{-1}). The PLA Virgin spectra is shown in Fig. 6. In PLA, the characteristic stretching frequencies for $-CH_3$ asymmetric, $-CH_3$ symmetric, and C-O are shown at 2997.50 cm−1 at 95.35%, 2921.48 cm−1 at 94.29%, and 1083.61 cm−1 at 42.33% respectively. The absorption peak 1748.17 cm−1 at 49.85% corresponding to its carbonyl groups. It has been determined that the bending frequencies of $-CH_3$ asymmetric and $-CH_3$ symmetric are 1452.04 cm−1 at 79.47% and 1358.16 cm−1 at 82.12% respectively.

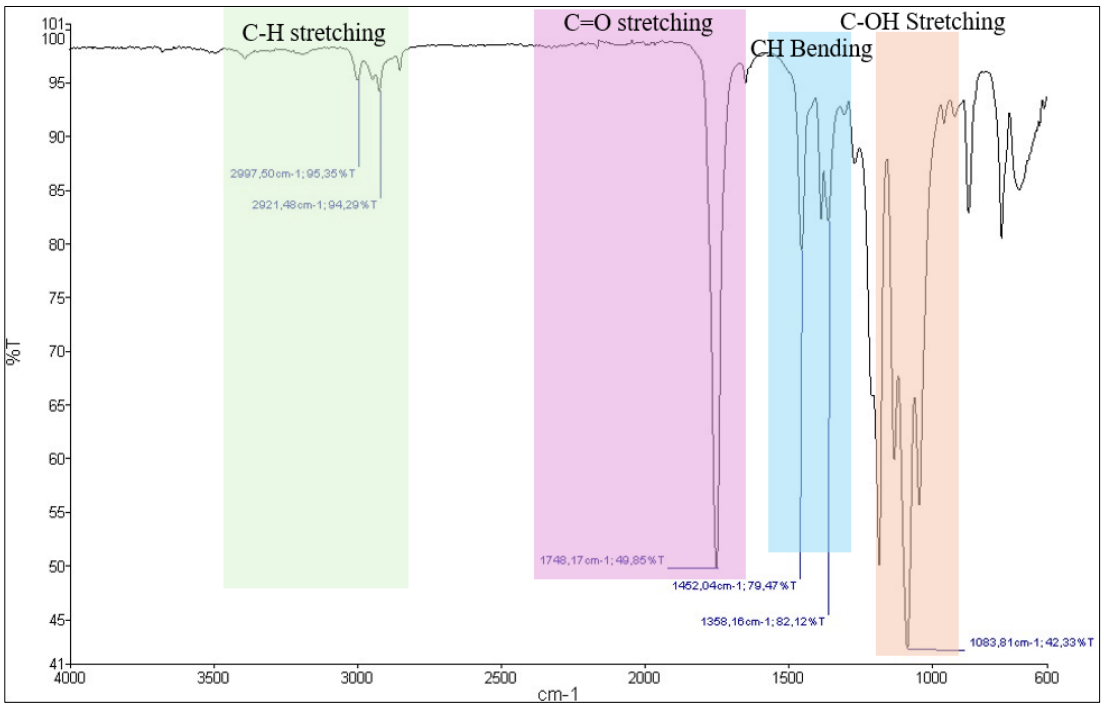

Fig. 6 FTIR spectra for PLA Virgin

FTIR spectroscopy was used for analyzing the different functional groups of HA powder. The results are displayed in Fig. 7. The FTIR spectrum displays every one of HA characteristic absorption peaks. Peaks from HAp are often contributed from phosphate groups. The distinct peaks located at 962.60 cm^{-1} at 74.09% and 1023.10 cm^{-1} at 74.09% and 12.58% correspond with the C-OH stretching vibrations of phosphate ($PO_4{}^{-3}$) group. This indicate that the primary molecular constituents of HA responsible for the infrared absorbance in the 600-1200 cm^{-1} range are the $PO_4{}^{-3}$[3].

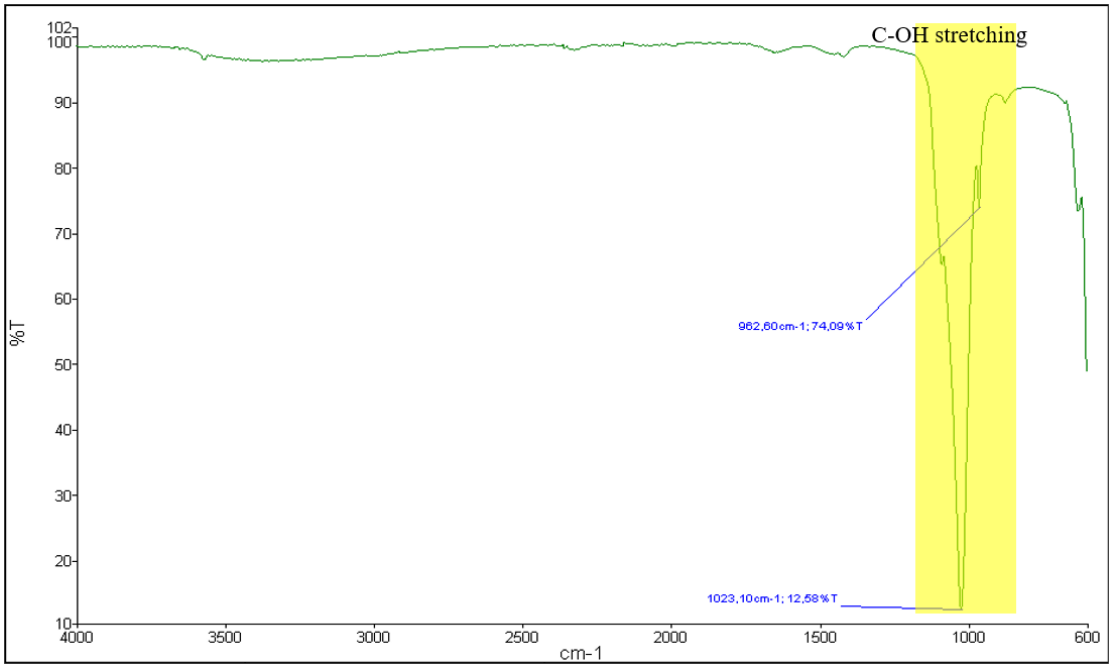

Fig. 7 FTIR Spectra for Hydroxyapatite (HA)

For PLA and HAp composites, three ratios which are 90/10, 80/20, and 70/30 are utilized. Fig. 8 illustrates variations in absorbance or the absence of specific peaks in FTIR spectra. These absorption peaks correspond to functional groups present in HAp and pure PLA.

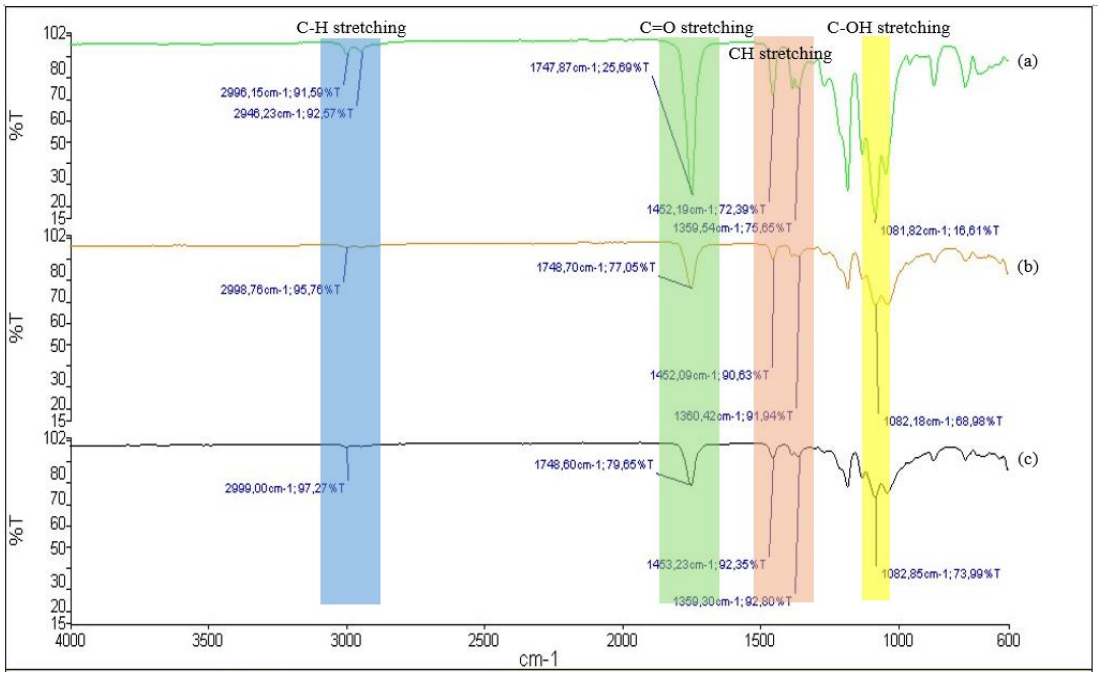

Fig. 8 FTIR Spectra for PLA and HAp (a) 90/10 (b) 80/20, (c)70/30

The FTIR spectra confirmed the presence of both PLA (organic) and HAp (inorganic) in all ratios. Figure 8 shows the IR spectra of composites-based hydroxyapatite at weight ratios of (a) 90/10 (b) 80/20, (c)70/30. The characteristic absorption bands of C-H bonds of methyl group of PLA are located at 2999 $\boldsymbol{cm^{-1}}$ and 2946 $\boldsymbol{cm^{-1}}$. The C=O and CH stretches are responsible for the absorption peaks located at 1748 and 1359 to 1453 $\boldsymbol{cm^{-1}}$, respectively. For phosphate ($\boldsymbol{PO_4{}^{-3}}$), the frequencies can be found in the range of 1082.85 to 1081.82 $\boldsymbol{cm^{-1}}$.

3.2 Analysis of Surface Roughness

Table 4 shows the surface roughness of PLA, HAp and PLA/HAp with different ratios. Two types of images will be captured, which are 2D and 3D.

Table 4 *Surface roughness of PLA, HAp and PLA/HAp with different ratio*

Samples	2D Images of AFM Surface Topography	3D Images of AFM Surface Topography
PLA Virgin	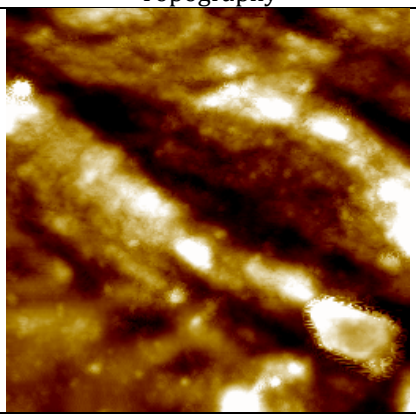	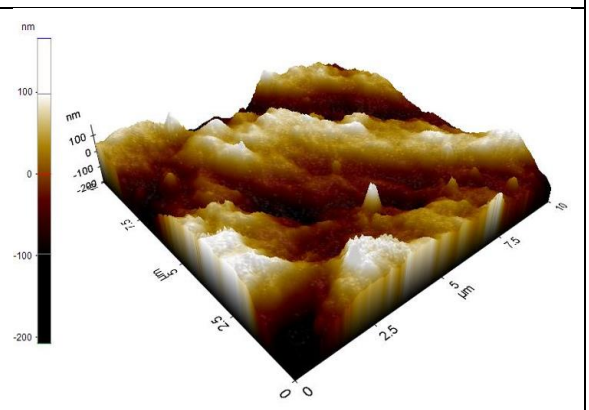

Hydroxyapatite (HAp)	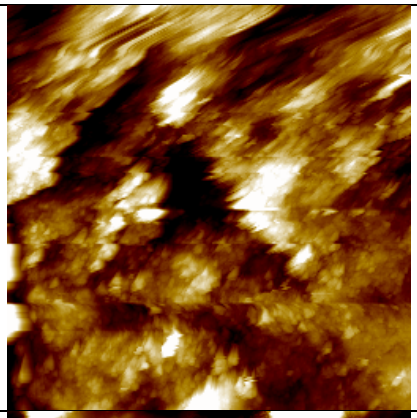	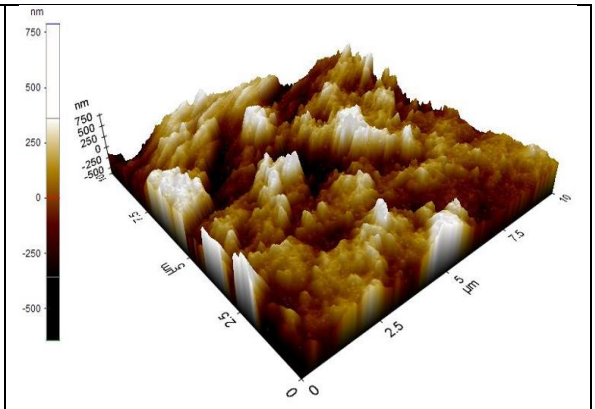
PLA/HAp 90/10	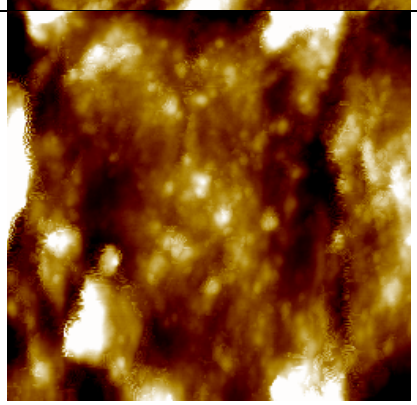	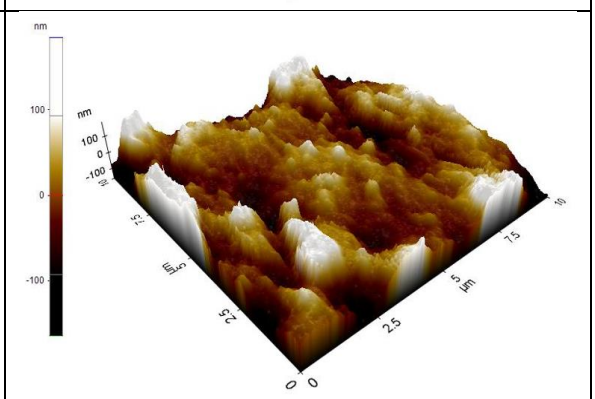
PLA/HAp 80/10	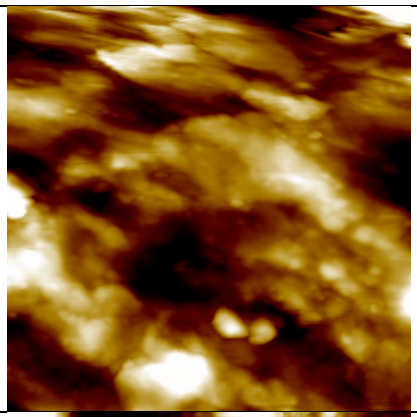	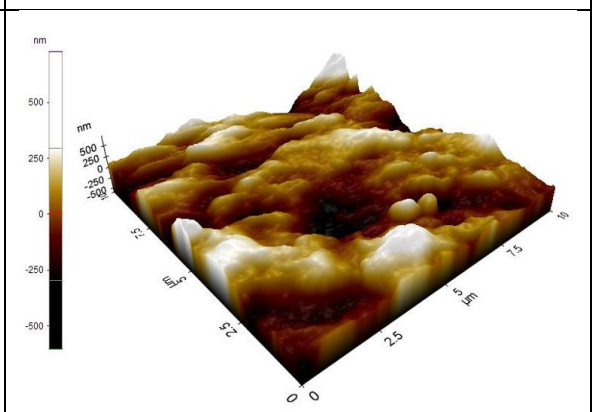
PLA/HAp 70/30	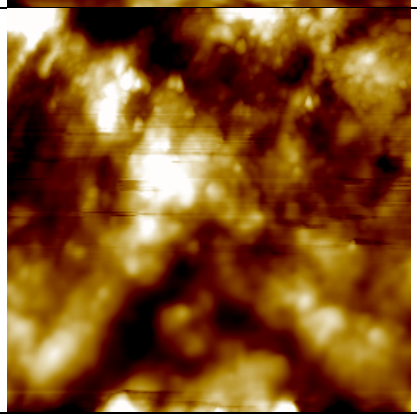	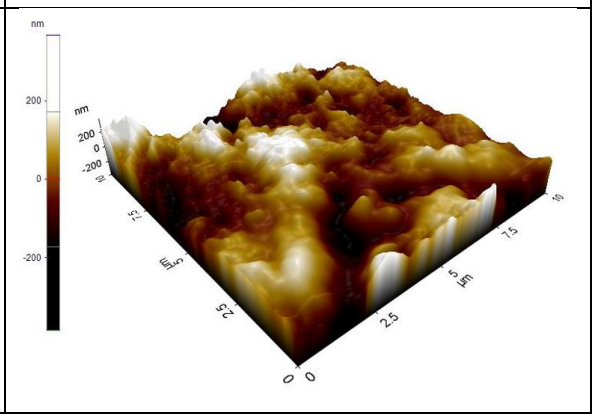

Table 5 *Tabulated the roughness parameters data for PLA/HAp.*

Roughness Parameters			
Samples	Roughness Peak to Valle, Rpv (nm)	Roughness root mean square, Rq (nm)	Roughness Average, Ra (nm)
PLA Virgin	276.245	36.937	29.108
Hydroxyapatite (HAp)	1433.542	183.088	143.477

PLA/HAp 90/10	349.133	47.358	35.617
PLA/HAp 80/10	1330.806	151.168	120.644
PLA/HAp 70/30	754.159	88.218	68.974

Pure HAp is significantly rougher than PLA Virgin across all parameters. As the content of HAp increases in the PLA/HAp composites, the roughness values increase which indicates that the addition of HAp increases surface roughness. The 90/10 blend appears to be the smoothest composite, while the 80/10 blend is the roughest. 70/30 blend has moderate roughness compared to the other blends

Surface roughness has an important significance in biomedical because it influences cell adhesion and proliferation. Surface roughness influences cells' initial adherence to the implant surface. Rougher surfaces have more surface area and micro-scale features, which improve cell adhesion and proliferation. Rough surfaces allow cells to attach, spread, and develop more effectively, which can improve the implant's integration with tissues nearby. [4]. Rough surfaces on bone implants improve osteointegration, which is the direct structural and functional connection between living bone and implant surface. HAp in the composite improves bioactivity and bone formation, and surface roughness is critical in this process. A rougher surface may stimulate bone development at the contact, resulting in faster and more robust healing of the implant site [5].

3.3 Microstructure Analysis

Two magnifications were used for characterization which is x500 and x1000. The HAp dispersion on the PLA matrix was observed at a 15 0kV accelerating voltage. The SEM images (Fig. 9(a-j)) illustrate the surface morphology of PLA Virgin, HAp, and composition of PLA/HAp. The distribution, amorphous physical structure, morphology of compatibilizers PLA Virgin can be observed using SEM as shown in Fig. 9 (a) and (b).

Figure 9 (c) and (d) show the morphology of the HAp in different magnification. It can be said that the surface of HAp is quite rough. In Fig. 4.5 (d), there are uneven size particles that can be detected. The grinding effect during preparation of sample may be the cause of the uneven size of the particles. This is also the effect agglomeration of HAp particles.

The first ratio that will be used will be 90% of PLA and 10% of HA. The result for this ratio is shown in Fig. 9(e) and (f). The figure showed that the HAp particles were distributed homogenously across the PLA's surface layer. PLA with 10% HAp infill was as smooth and homogeneous in structure.

The next ratio was 80% of PLA and 20% of HA. As shown in Figure 9 (g) and (h), HAp intact well on the surface of PLA's. The elements of PLA and HAp are still present due to the success of the blending process.

The last ratio that is used was 70% of PLA and 30% of HA. The result for this ratio will be as shown in Fig. 9 (i) and (i). PLA with 30 wt.% of HAp still filling very smoothly and the distribution is homogeneous. Since the PLA amount is reduced, the contribution of HAp is more significant. The amount of PLA affected the particle size based on the SEM results, and it also showed that when the amount of PLA decreases, the size of the HAp particle increases. This is most likely because higher amounts cause HAp particles to disperse in between the PLA network and prevent their aggregation [6].

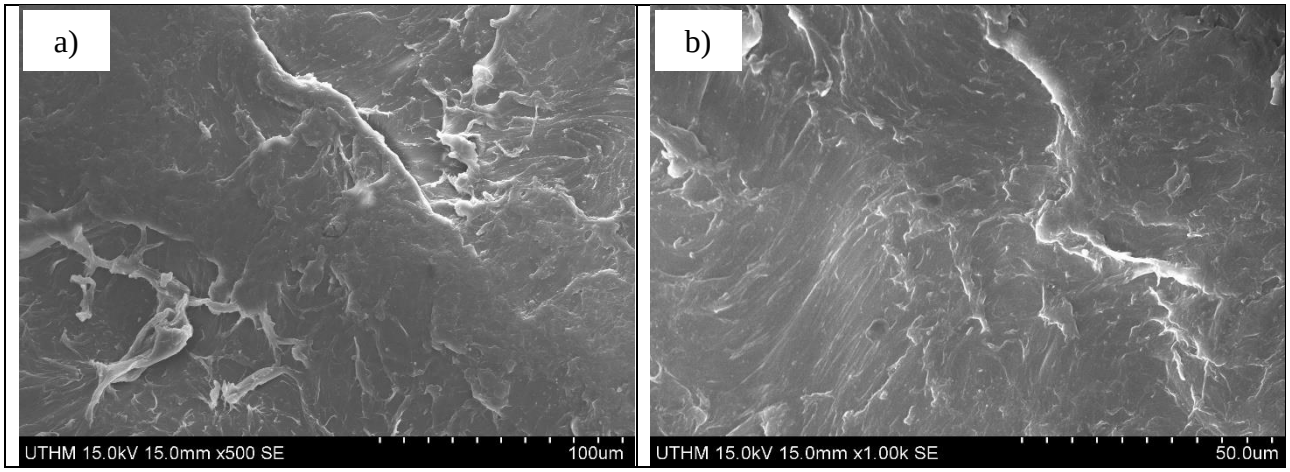

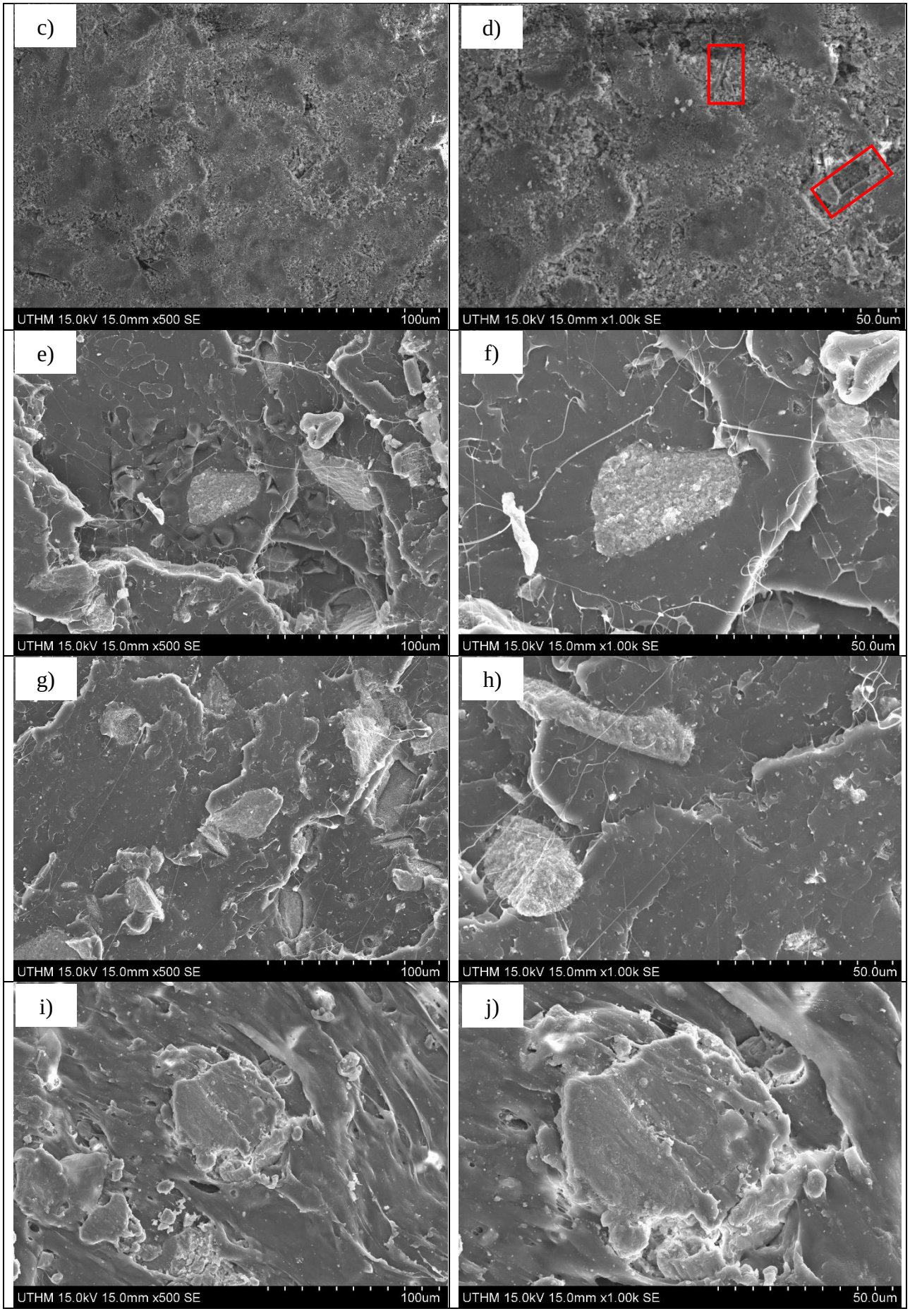
c)
UTHM 15.0kV 15.0mm x500 SE 100um
d)
UTHM 15.0kV 15.0mm x1.00k SE 50.0um
e)
UTHM 15.0kV 15.0mm x500 SE 100um
f)
UTHM 15.0kV 15.0mm x1.00k SE 50.0um
g)
UTHM 15.0kV 15.0mm x500 SE 100um
h)
UTHM 15.0kV 15.0mm x1.00k SE 50.0um
i)
UTHM 15.0kV 15.0mm x500 SE 100um
j)
UTHM 15.0kV 15.0mm x1.00k SE 50.0um

Fig. 9 SEM Images for PLA, HAp, PLA and HAp at x500 and x1000 Magnifications

For Elementary Chemical Composition of PLA Virgin. The elemental compositions obtained from EDS of PLA Virgin are shown in Fig. 10(a). Based on the result, there is presence of Carbon (C) and Oxygen (O) in PLA Virgin.

The elemental compositions obtained from EDS for HAp are shown in Fig.10(b). There are various elements that can be presence in HA such as Calcium (Ca), Carbon (C), Oxygen (O), Magnesium (Mg) and Phosphorus (P). Based on the result of previous study conducted, Magnesium (Mg) detected in this natural HAp which indicated the traces element that enhance bone growth [7].

Based on EDS result in Fig. (c), the elemental compositions that are present after PLA and HAp blended are Calcium (Ca), Carbon (C), Oxygen (O), Magnesium (Mg) and Phosphorus (P). This indicates that PLA and HAp are successfully blended since the element both are still presence. The elements of PLA/HAp are still presence due to it not chemically reacting to form new compounds but rather physically blended.

Data in Fig. 10 (d) represence the elemental compositions that are present after PLA and HAp blended with ratio 80/20. There are Calcium (Ca), Carbon (C), Oxygen (O), Magnesium (Mg) and Phosphorus (P).

Fig. 10 (e)shows the elemental compositions that are present after PLA and HAp blended. Elements such as Carbon (C), Oxygen (O), Magnesium (Mg), Phosphorus (P) and Calcium (Ca) can be found in this ratio. It can be said that the elements that originally consists in PLA and HAp are still well maintained after the process of blending settle.

a)

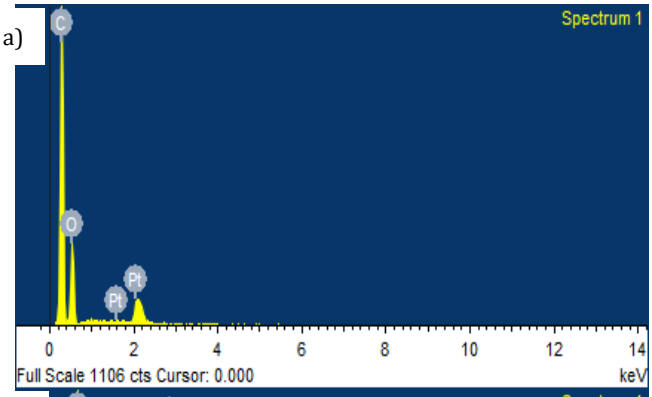

Element	Weight%	Atomic%
C K	61.69	71.46
O K	32.33	28.11
Pt M	5.99	0.43
Totals	100.00	

b)

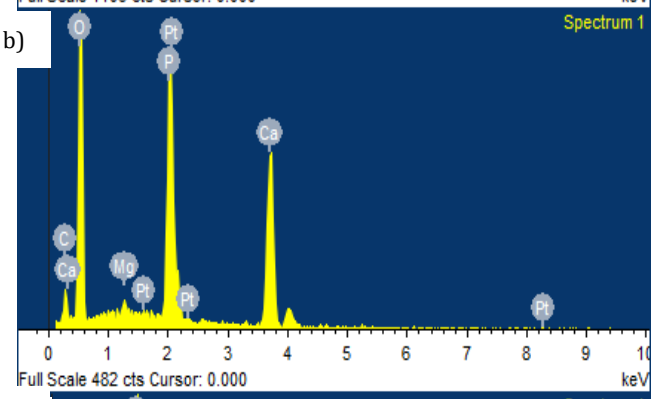

Element	Weight%	Atomic%
C K	7.32	12.43
O K	53.87	68.71
Mg K	0.60	0.50
P K	13.36	8.80
Ca K	17.19	8.75

c)

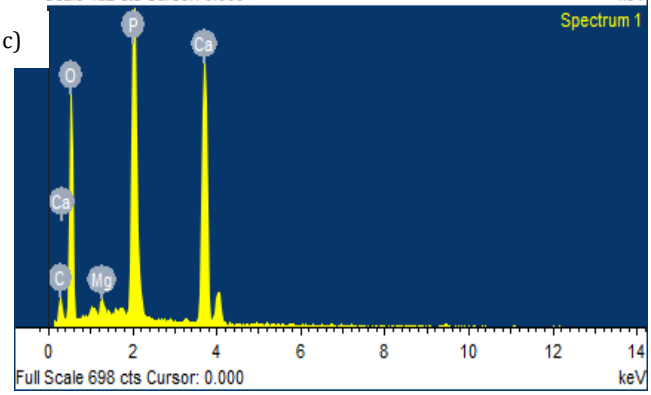

Element	Weight%	Atomic%
C K	7.14	12.14
O K	49.41	63.04
Mg K	0.77	0.65
P K	16.33	10.76
Ca K	26.34	13.42

d)

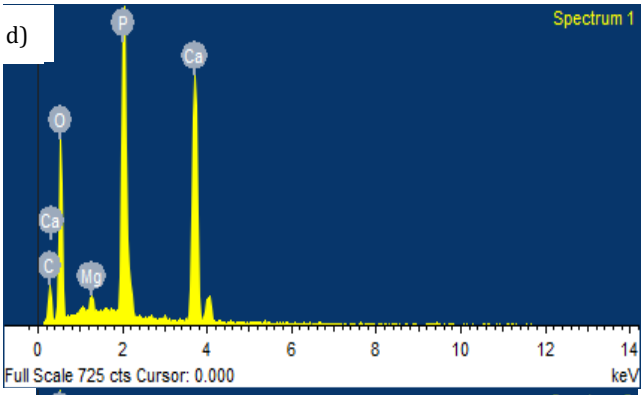

Element	Weight%	Atomic%
C K	11.12	18.63
O K	44.96	56.55
Mg K	0.91	0.76
P K	16.72	10.86
Ca K	26.29	13.20

e)

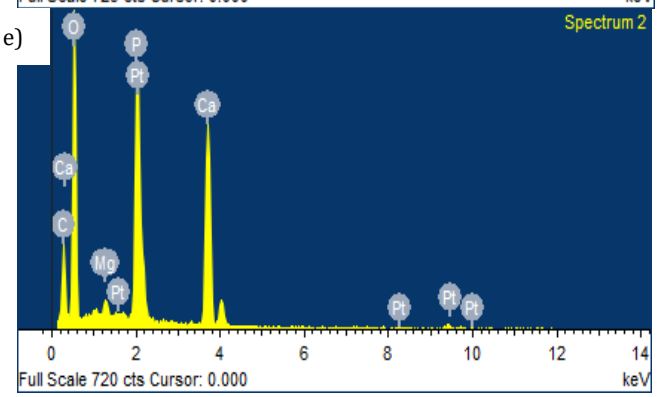

Element	Weight%	Atomic%
C K	14.25	23.18
O K	49.41	60.32
Mg K	0.72	0.58
P K	10.51	6.63
Ca K	17.48	8.52

Fig. 10 EDS Spectra (a)PLA Virgin (b)HAp (c)PLA/HAp 90/10 (d)PLA/HAp 80/20 (e)PLA/HAp 70/30

To identify and characterize the crystalline phases present in HAp, X-ray diffractometry (XRD) method is used since the HAp is in powder form. The powder is pressed to produce a tablet to facilitate the XRD process. Figure 4.6 shows the XRD result for HAp, which reveals the characteristic peak. The XRD evaluation shows that the sample is primarily composed of hydroxyapatite (HAp) with high crystallinity. This is supported by large peaks at 25.9°, 31.8°, 32.9°, 34.1°, and 39.9°, which confirmed the presence of HAp. The existence of additional peaks that match whitlockite shows that the sample contains secondary phases. This could be due to contaminants or the partial conversion of HAp into other calcium phosphate phases during synthesis or processing[8]. The overall crystallinity and phase composition are crucial to the material's performance in biomedical applications such as bone growth enhancement. Fig.11 shows XRD result of HAp.

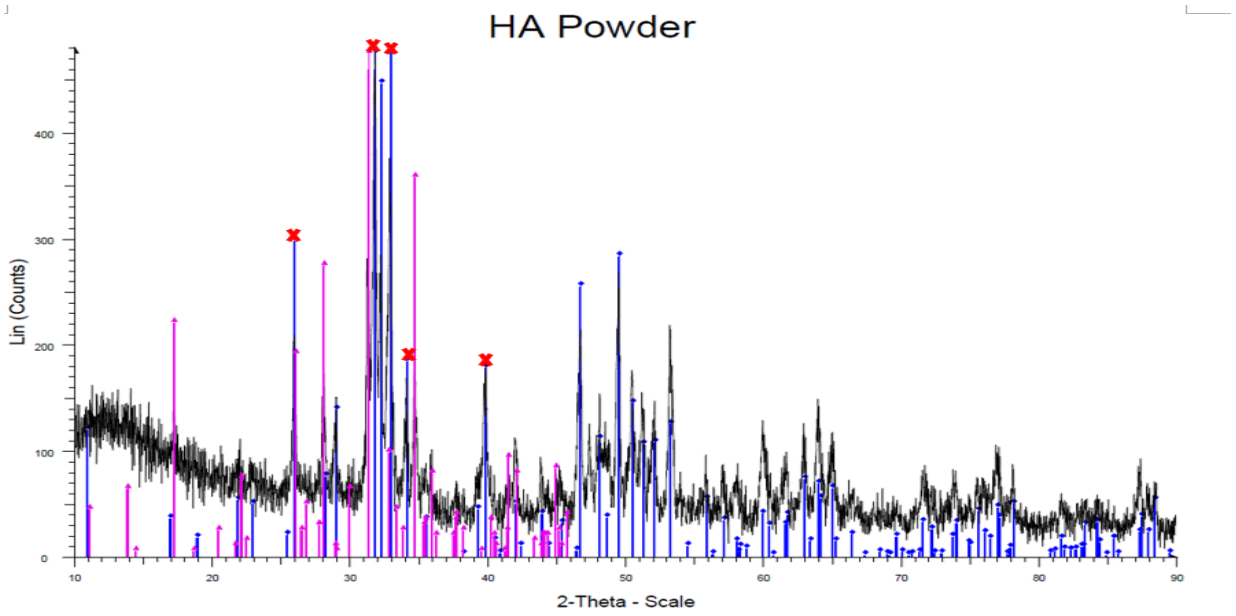

Fig. 11 XRD result of HAp

4. Conclusion

In conclusion, this study successfully investigated the mechanical properties, characterization, and physiochemical analysis of PLA/HAp filaments, highlighting their possible uses in medical applications. The main objectives were met through a series of comprehensive tests and analyses. FTIR analysis confirmed the presence of chemical bonding within the composites, identifying characteristic peaks for both PLA and HAp, which indicated successful integration of the two materials. This bonding is crucial for the performance of the PLA/HAp, especially in applications requiring tissue engineering, dental implants, and orthopedic applications.

Surface roughness analysis using AFM revealed that pure HAp exhibited significantly higher roughness compared to PLA Virgin. As the HAp content increased in the PLA/HAp composites, there was a corresponding increase in surface roughness. This can be proved as the highest Roughness Average (Ra) that obtained in PLA/HAp is 68.974 mm. This enhanced roughness can positively affect cell adhesion and proliferation, making these composites particularly promising for biomedical applications where surface texture plays a critical role in tissue integration and regeneration.

Microstructural analysis using SEM-EDS provided detailed insights into the distribution of HAp within the PLA matrix. The presence of elements such as Carbon (C), Oxygen (O), Calcium (Ca), Magnesium (Mg) and Phosphorus (P) was confirmed and well maintained after the blending process is done, which are indicative of the composite's composition. Additionally, XRD analysis validated the crystalline phases present in HAp, demonstrating its high crystallinity. These findings are essential for understanding the material's structural integrity and performance under various conditions.

Mechanical testing using UTM demonstrated significant enhancements in the tensile, bending, and flexural properties of the PLA/HAp composites compared to pure PLA. The addition of HAp improved the elastic modulus and tensile strength, making the composites more robust and suitable for demanding applications. The results from flexural and bending tests further corroborated these findings, showing improved resistance to deformation and failure. Overall, the incorporation of HAp into PLA not only enhances its mechanical properties but also makes it a viable material for advanced biomedical applications, where both mechanical strength and biocompatibility are critical.

Acknowledgement

The authors wish to extend their deepest gratitude for the financial support provided by Universiti Tun Hussein Onn Malaysia and the UTHM Publisher's Office through Publication Fund E15216. They also thank the Faculty of Mechanical and Manufacturing Engineering at Universiti Tun Hussein Onn Malaysia for their support.

Conflict of Interest

Authors declare that there is no conflict of interests regarding the publication of the paper.

Author Contribution

This study was originated and designed by [Jerome Tunggat Anak Kasin] who also performed the data analysis. [Prof. Dr. Maizlinda Izwana Binti Idris] made substantial contributions to the interpretation of the results and offered essential revisions.

References

[1] James Bricknell, "Best 3D Printing Filament in 2023." Accessed: Nov. 04, 2023. [Online]. Available: https://www.cnet.com/tech/computing/best-3d-printing-filament/

[2] A. P. Marzuki, M. A. M. Nasir, F. M. Salleh, M. H. Ismail, B. I. S. Murat, and M. Ibrahim, "Initial Study on Rheological Behaviour of Hydroxyapatites/Polylactic Acid Composite for 3D Printing Filament," *International Journal of Automotive and Mechanical Engineering*, vol. 21, no. 1, pp. 11064–11073, 2024, doi: 10.15282/ijame.21.1.2024.10.0856.

[3] Md. H. M. K. A. S. alam, M. A. Gafur, "Chemical Characteristics of Hydroxyapatite from Oyster Shell by Thermo-Chemical Process," *Int J Innov Res Sci Eng Technol*, vol. 04, no. 07, pp. 5039–5047, Jul. 2015, doi: 10.15680/ijirset.2015.0407002.

[4] A. Zareidoost, M. Yousefpour, B. Ghasemi, and A. Amanzadeh, "The relationship of surface roughness and cell response of chemical surface modification of titanium," *J Mater Sci Mater Med*, vol. 23, no. 6, pp. 1479–1488, Jun. 2012, doi: 10.1007/s10856-012-4611-9.

[5] M. P. Bernardo *et al.*, "PLA/Hydroxyapatite scaffolds exhibit in vitro immunological inertness and promote robust osteogenic differentiation of human mesenchymal stem cells without osteogenic stimuli," *Sci Rep*, vol. 12, no. 1, Dec. 2022, doi: 10.1038/s41598-022-05207-w.
[6] N. M. Mustaza *et al.*, "Influence of Hydroxyapatite Particle Size on the Flowability of PLA/HA Filament," *Journal of Mechanical Engineering*, vol. 21, no. 2, pp. 159–179, 2024, doi: 10.24191/jmeche.v21i2.26261.
[7] A. Zastulka *et al.*, "Recent Trends in Hydroxyapatite Supplementation for Osteoregenerative Purposes," *Materials*, vol. 16, no. 3. MDPI, Feb. 01, 2023. doi: 10.3390/ma16031303.
[8] H. L. Jang, H. K. Lee, K. Jin, H. Y. Ahn, H. E. Lee, and K. T. Nam, "Phase transformation from hydroxyapatite to the secondary bone mineral, whitlockite," *J Mater Chem B*, vol. 3, no. 7, pp. 1342–1349, Feb. 2015, doi: 10.1039/c4tb01793e.